Fabrication of Honeycomb Polyvinyl Butyral Film Under Humidity Provided by Super Saturated Salt Solutions

Ruimin Zhang, Jinwei Wang, Minjia Wang, Yedong He

Institute of Advanced Materials and Technology, University of Science and Technology Beijing, Beijing 100083, China

Received 20 December 2010; accepted 27 April 2011
DOI 10.1002/app.34795
Published online 5 October 2011 in Wiley Online Library (wileyonlinelibrary.com).

ABSTRACT: We introduce a novel method for making breath figure arrays (BFAs) on polyvinyl butyral (PVB) films under humidity by putting the dip coated samples inside a chamber filled with supersaturated salt solutions. With the increase in humidity or retention time, multiple porous films with bigger pore sizes and wider size distributions are generally obtained, resulting from the coalescence of the following-up water drops. The presence of nitrogen flow accelerates the evaporation of solvents and vapor, thus increases the elastic interaction among water droplets such that films with smaller pores can be obtained. Compared to PVB/ethyl acetate solution, it is easier to obtain a film with regular honeycomb pattern by using PVB/chloroform solution. Its lower boiling point makes it evaporate faster to increase temperature gradient between film surface and the atmosphere; while its higher density makes it provide stronger support to maintain the shape of water droplets. In this study, the solubility of polymer in solvents is initially proposed to explain the BFAs formation. Higher mobility of polymer chains in a good solvent increases chances of its polar groups to interact with water droplets, thus increases the possibility of regular arrangements of water droplets on the film. © 2011 Wiley Periodicals, Inc. J Appl Polym Sci 124: 495–500, 2012

Key words: thin films; interfaces; scanning electron microscopy (SEM); polyvinyl butyral

INTRODUCTION

Porous polymer films have attracted much attention because of their potential applications in the fields of catalyst and carrier,[1] biological culture media,[2,3] membranes for separation or adsorption,[4,5] photoelectric device,[6] and so on. So far, many methods have been developed to fabricate porous polymer films, such as the monodisperse colloidal crystal particles template method,[7,8] the emulsion and surfactant template method,[9,10] the microphase-separated block copolymer template method,[11,12] and the biological template method.[13] In 1994, François and coworkers[14] obtained the ordered honeycomb micropore films by spreading poly(para-phenylene)-block-polystyrene (PPP-PS) and star polystyrene solution on a smooth substrate under high humidity condition, and it was called breath figure method (BFs). Since then, the merit of obtaining controllable micropores with desirable size and shape by this method has given rise to the interests in developing various techniques, including solid substrates expansion method,[3,15] on-water spreading method,[16] emulsions method,[17] and dip-coating method.[18]

Correspondence to: J. Wang (wangjw@ustb.edu.cn).

Journal of Applied Polymer Science, Vol. 124, 495–500 (2012)

Because of its easier operation, breath figure method (BFs) has been one of the most popular methods to fabricate porous polymer film in recent years. Under humid conditions, solvent evaporation cools the solution surface of polymer in solvent during which water vapor in the atmosphere condenses and water droplets are formed at the interface of the polymer solution. Then, water droplets interact with one another and finally obtain an ordered lattice. Finally, when the solvent and water are completely evaporated, traces of water droplets remain in the polymer film and become pores with a honeycomb structure. The key process to this method is to form stabilizing condensed water droplets on the volatile polymer solution.[19] The detailed mechanism of BFAs formation on polymers is still under disputation, however, apart from the processing parameters such as humidity, temperature, solution concentration, and retention time, polymer structures and solvent characteristics are considered two of the most crucial interior factors in influencing the pore formation.

Initially the materials used for honeycomb film were focused on star polymer, polystyrene with the polar functional group ends and segment copolymers of polystyrene.[14,20] So far, polymer materials including rod-coil block copolymer,[21] comb polymer,[22] linear polymer,[23] polymer-crown ether block copolymer,[24] amphiphilic copolymer,[25] polyion complexes,[26] and hyper branched polymers[27] have been reported to make honeycomb films in the literatures.

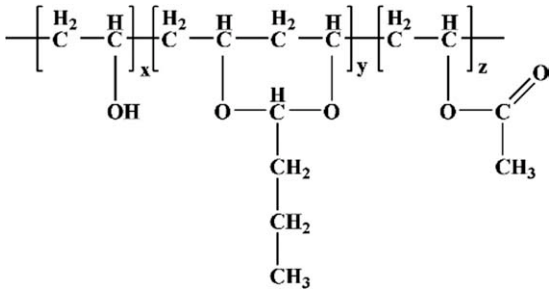

Figure 1 Chemical structure of polyvinyl butyral (PVB) (provided by the supplier).

Generally, carbon disulfide (CS_2) should be first considered as the solvent for star and block polystyrenes, carboxyl-terminated polystyrenes as well as an unknown polymer which are as materials of casting film, while chloroform is a good choice when the polymer is non-end-group-functionalized PS, and nitrocellulose/amyl acetate solution can be used to make honeycomb micopore film by breath figure.[23,28] Usually good self-assembled honeycomb film can also be obtained using benzene, toluene, or xylene as solvents.[28] In addition, Park and Kim[29] have obtained the ordered honeycomb film by THF solution of cellulose acetate-butyrate, carboxylate-terminated PS, and poly(methyl methacrylate) by spin coating method in a dry atmosphere, and meanwhile the water was supplied in the solvent.

So far, the relationships among various factors in influencing the shape and size of the honeycomb structure are still not clear. In this article, we initially fabricate breath figure patterns on polyvinyl butyral (PVB), an amphiphilic polymer with hydrophobic main chain and hydrophilic side chains which has been used in the fields of coating, solar cell, and electronic fields due to its excellent mechanical strength, film forming ability, and transpancy,[30,31] to make porous films by putting the dip-coated samples into the humidity condition controlled by the super saturated salt solutions, their pore size and distribution related to the humidity, solvent, and PVB structure are discussed; hopefully this porous film can be a good choice used as catalyst, protein, or diode material carriers,[1–3] membranes for separation and adsorption,[4,5] and so on. Worthy to mention, the relative humidity is controlled by the super saturated salt solutions (see "the Scale of Relative Humidity of Air Certified Against Saturated Salt Solution," OIML R121, edition 1996), which is more convenient and accurate, and better reproducible compared to those water vapor, water bubble and moist air flow methods in the literatures, avoiding the fluctuation in humidity since the continuous operations of humidifier, bubbler, and valve of air may result in the increase in humidity, and conversely, their longer time pause may result in the decrease in humidity.

EXPERIMENTAL

Materials

Polyvinyl butyral (PVB) (AR, M_n = 98,400, polydispersity index (PDI) = 1.34, the butyral content 45.0–49.0% (wt%), water content less than 0.2 wt %), purchased from Sinopharm Chemical Reagent, China, its chemical structure is shown in Figure 1. Chloroform (AR) and ethyl acetate (AR), supplied by Sinopharm Chemical Reagent, China, distilled before use. Sodium bromide (AR, NaBr), sodium chloride (AR, NaCl), and potassium sulphate (AR, K_2SO_4), purchased from Beijing Chemical Corporation, and used as received.

Films preparation

As shown in Figure 2, rectangular chambers equipped with a tight cover, several hooks for the sample holding and two nozzles for nitrogen flow passing through were used to make the BFAs films. Before putting the dip-coated samples inside, it had to be charged 1/3 of the volume with super saturated NaCl, NaBr, or K_2SO_4 solutions and stayed for 30 min at 30°C. The humidity of these super saturated solutions can be precisely controlled at (56.0 ± 0.4)% for NaBr, (75.1 ± 0.2)% for NaCl, and (97.0 ± 0.4)% for K_2SO_4, respectively.

Dipping solutions were made by dissolving 4.0 g PVB in 100.0 mL chloroform or ethyl acetate and stored at least 2 h before using. Cover glasses (20 mm × 20 mm) washed by alcohol and then DI water were used as substrates. After drying, the clean cover glass was dipped in the PVB solutions for 30

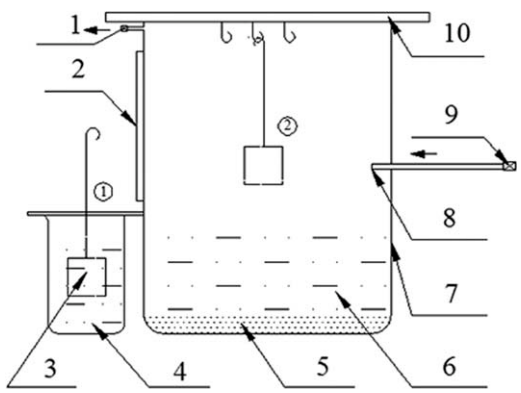

Figure 2 The schematic plot of test apparatus: 1, 9—N_2 valve; 2—door; 3—cover glass; 4—PVB solution; 5—salt; 6—super saturated salt solutions; 7—rectangular chamber; 8—N_2 flow passing through; 10—tight cover. 1 dip-coating sample, 2 putting the sample in the humidity condition.

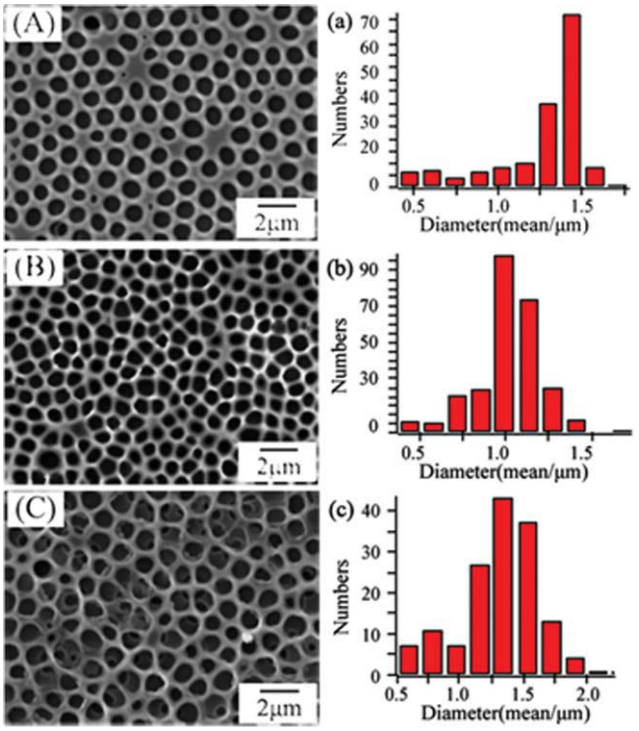

Figure 3 SEM surface images and their average pore diameter distribution diagrams of the films formed by PVB/chloroform solution (0.04 g mL^{-1}) at humidity of 75.1% ± 0.2% at retention time: (A, a) 20 s; (B, b) 30 s; (C, c) 60 s. [Color figure can be viewed in the online issue, which is available at wileyonlinelibrary.com.]

s, pulled out and then immediately transferred into the rectangular chamber to fabricate porous films. When necessary, the valve remained open to purge N_2 flow at velocity of 1 L min^{-1} before putting the dip-coated samples inside the chamber. The retention time (time of samples staying in the chamber) of these samples was set for 20, 30, and 60 s.

Morphology examination and image analysis

Surface topography and lateral domain arrangement were examined by scanning electron microscopy (SUPRA55, Germany) working in 10 KV, in lens signal mode, and the samples were sputtered by carbon before the SEM measurement. The average pore diameters and distributions were inspected and measured by using the Image-pro Plus software (Media Cybernetics, America).

RESULTS AND DISCUSSION

Breath figure patterns under different retention time

Figures 3 and 4 show the SEM images and their corresponding pore distribution analysis diagrams of films made from PVB/chloroform and PVB/ethyl acetate in a humidity of 75.1% ± 0.2% for 20, 30, and 60 s, respectively. At a retention time of 20 s, the sizes of the pores formed on PVB/chloroform films are around 1.35 μm with very narrower size distribution [Fig. 3(A,a)], while the pore sizes of PVB/ethyl acetate films are in a broader range from 1.0 to 4.0 μm [Fig. 4(A,a)]. When they stay for 30 s, most of the pore sizes of PVB/chloroform films become smaller and the walls among pores get thinner [Fig. 3(B,b)]; the pore size and distribution of PVB/ethyl acetate film however does not show much changes except for the appearance of multilayer pores [Fig. 4(B,b)]. If both of the samples stay longer for 60 s, their pore sizes grow bigger with a much broader size distribution, and much more multilayer pores are both observed [Figs. 3(C,c) and 4(C,c)].

Fewer water droplets are condensed on the liquid film at short retention time in the humidity condition, and the condensed water droplets are sparsely accumulated, the walls among water droplets are relatively thicker, which make the repelling force between adjacent water droplets weaker until the film is cured. In this case, the surface tension[25,32] between the polymer and water droplets plays a leading role, the droplets are randomly arranged, consequently, leaving pores appear as the size of droplets when the film is cured [Figs. 3(A) and

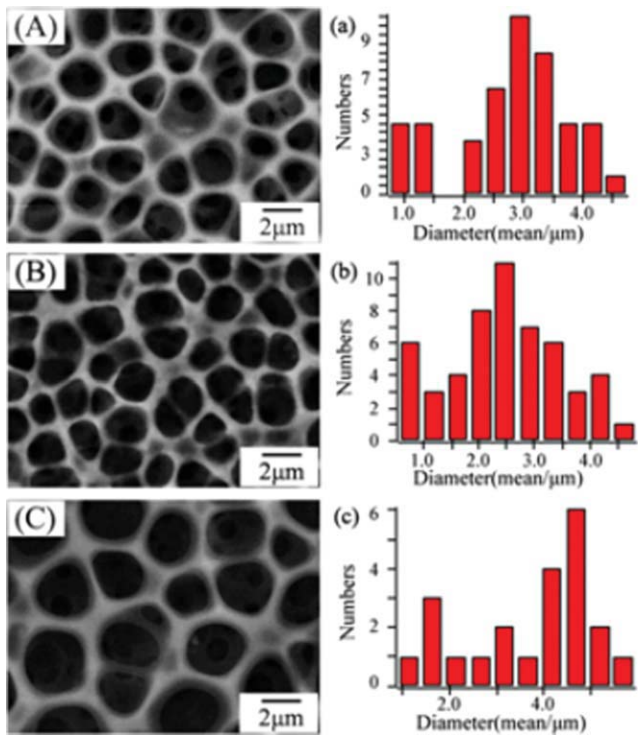

Figure 4 SEM surface images and their average pore diameter distribution diagrams of the films formed by PVB/ethyl acetate solution (0.04 g mL^{-1}) at humidity of 75.1% ± 0.2% at retention time: (A, a) 20 s; (B, b) 30 s; (C, c) 60 s. [Color figure can be viewed in the online issue, which is available at wileyonlinelibrary.com.]

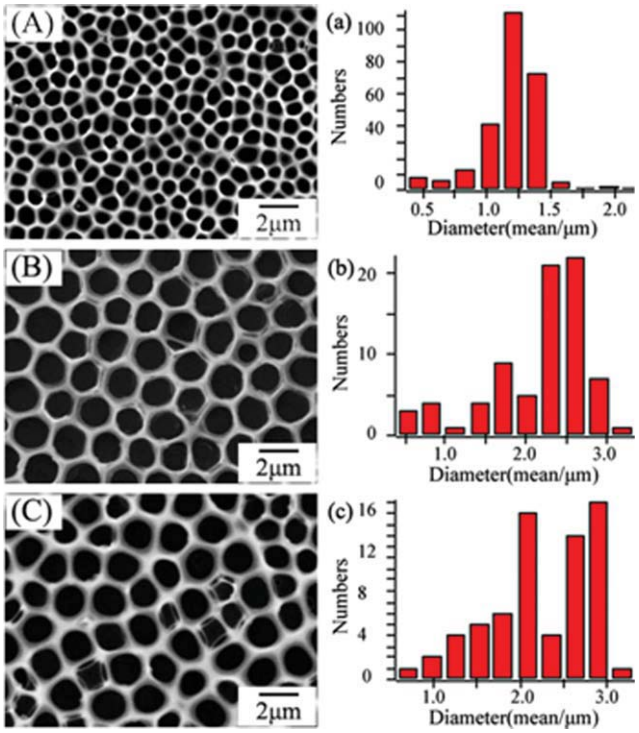

Figure 5 SEM surface images and their average pore diameter distribution diagrams of the films formed by PVB/chloroform solution (0.04 g mL^{-1}) at humidity of (A, a): RH 56.0% ± 0.4%, (B, b): RH 75.1% ± 0.2%, (C, c): RH 97.0% ± 0.4% for 30 s. [Color figure can be viewed in the online issue, which is available at wileyonlinelibrary.com.]

4(A)]. With the increase in retention time, more water droplets condensing on the film surface makes the walls among water droplets become thinner, which results in the increase in the repelling force among adjacent water droplets.[25,32] As a result, pores density increases and pore shape grows more regular [Figs. 3(B) and 4(B)]. However, with the elongation of retention time, the liquid film surface would be covered by excessive condensed water droplets; meanwhile, temperature gradient between the film and water droplets is dispelled, the thermocapillary convective motion in and between the two bodies of fluid also disappear; when the time of interaction between the droplets is more than the time required for the vapor to escape the interstices, droplets wouldn't be able to interact elastically and lead to the coalescence of water droplets.[31] Hence the size of pores grows bigger, and multilayer of pores appears on the films [Figs. 3(C) and 4(C)]. The multilayer phenomena were initially considered to be influenced by the solvent density and only solvents that were less dense than water resulted in the formation of multiple pores,[33] while in some other later studies, multilayer pores were obtained when casting BFAs from CS_2.[34] In our case, both ethyl acetate (less dense than water) and chloroform (denser than water) have resulted in the formation of multilayer pores. It may be concluded that at certain humidity the multilayer pore formation is determined by the retention time rather than the density of solvents.

Breath figure patterns under different humidity

To investigate the effect of relative humidity on BFAs formation on PVB films, we precisely controlled the relative humidity at 56.0% ± 0.4%, 75.1% ± 0.2%, and 97.0% ± 0.4%, respectively provided by super saturated salts solutions, which correspond to the low, mild, and high humidity values as most of the literature used. The surface images and pores size distribution of the films at retention time of 30 s are shown in Figures 5 and 6, respectively.

At a humidity of 56.0% ± 0.4% by using PVB/chloroform, the relatively regular pores are observed in a diameter of around 1.0–1.5μm with narrow size distribution [Fig. 5(A,a)]. When the relative humidity is increased further to 75.1% ± 0.2%, the pore sizes grow bigger mostly in a diameter of 2.5 μm and highly ordered pores are generated [Fig. 5(B,b)]. When the humidity is at 97.0% ± 0.4%, the pore sizes are around 2.0–3.0 μm, which are a little bigger than those of samples at 75.1% ± 0.2%, respectively, and irregular shapes appear because of the

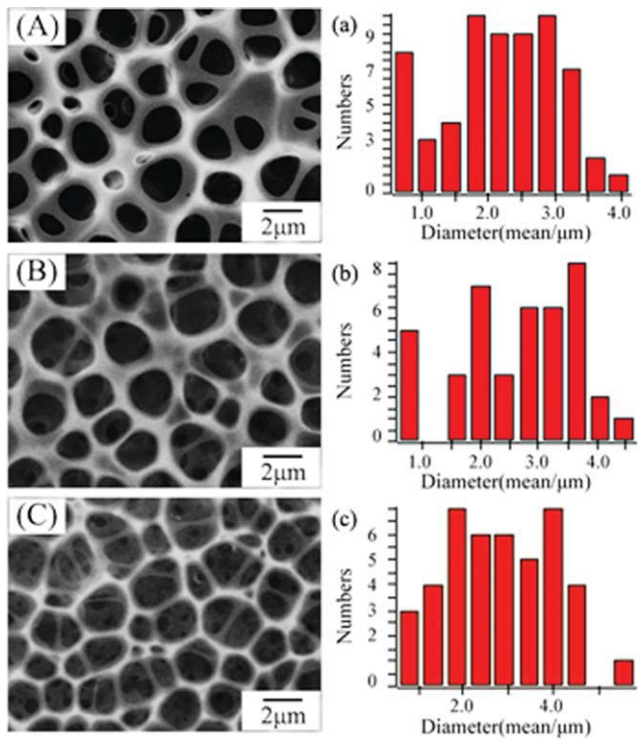

Figure 6 SEM surface images and their average pore diameter distribution diagrams of the films formed by PVB/ethyl acetate solution (0.04 g mL^{-1}) at humidity of (A, a): RH 56.0% ± 0.4%, (B, b): RH 75.1% ± 0.2%, (C, c): RH 97.0% ± 0.4% for 30 s. [Color figure can be viewed in the online issue, which is available at wileyonlinelibrary.com.]

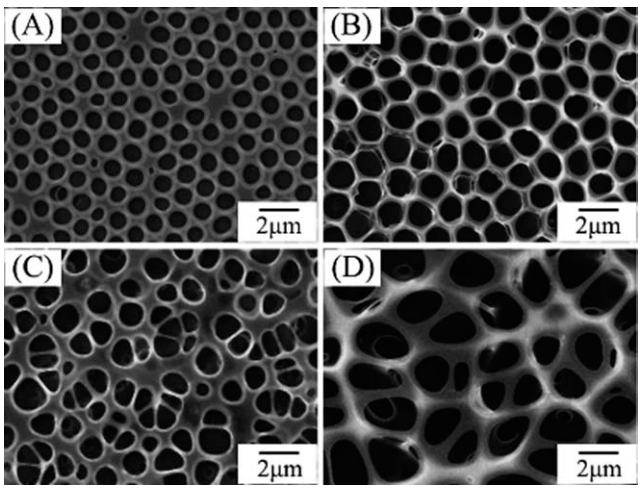

Figure 7 SEM surface images of the film made by PVB/chloroform solution (0.04 g mL^{-1}) (A,B) and PVB/ethyl acetate solution (0.04 g mL^{-1}) (C,D) with (A,C) and without (B,D) nitrogen airflow, respectively under humidity of 75.1% ± 0.2%.

coalescence of droplets under much higher humidity [Fig. 5(C,c)]. For BFAs obtained from PVB/chloroform, bigger pore sizes are obtained by increase the humidity, similar trend was found in the results of polystyrene/toluene system as reported by Li et al.[19] With the increase in humidity, more droplets are condensed on the surface of casting solution and sufficient follow-up droplets are provided to ensure the pore growth; the droplets sink into the solution in a short period of time, and the viscosity of solution increases with the evaporation of the solvent to stabilize the water droplets.[23] On the other hand, the polar side chain of PVB may have a tendency to concentrate around water droplets to slow down the diffusion of water droplets, resulting in the regular pattern formation [Fig. 5(B)].

However, as shown in Figure 6, at the three humidity values by using ethyl acetate as a solvent, irregular multilayer pores are observed on all the films, while the pore size and distribution remain almost unchanged with the increase in humidity. The interactions among solvent, polymer and water droplets may be crucial factors in determining the BFAs patterns, which will be discussed later.

Influence of the nitrogen airflow on the pore sizes and shapes

The nitrogen airflow strongly affects the evaporation rate of the solvents and in turn changes the BFAs patterns.[33] At the presence of nitrogen airflow, films with smaller pores and thicker walls, and the number of pores per unit of surface is generated [Fig. 7(A,C)]. In the breath figure method, the water vapor is condensed to form water droplets while the solution surface is cooled by the evaporation of the solvents.[15] Therefore, the nitrogen airflow accelerates the flow of humid atmosphere and the evaporation of the solvents,[33] the shorter interacting time between the droplets and polymer solutions results in the formation of smaller pores. It has recognized that such behavior is driven by a thermocapillary convective motion in and between the two bodies of fluid.[33,35] In this case, solvent volatilizing and water droplets condensing make the temperature gradient between the film and water droplets increase, which results in the increase in the thermocapillary convective motion, thus stabilize the condensing water droplets and also avoid their coalescence on the polymer solution surface, accordingly, the possibility to form multilayer pores also reduces.

Another hypothesis beyond thermocapillarity may be also reasonable.[33] In this situation, the water droplets are kept apart by elastic interaction during solvent evaporating, thus forming walls to separate the droplets. Once the interacting time between the droplets is less than that required for the vapor escaping from the interstices, the elastically interacting droplets restrains their coalescence.

Influence of the solvent on BFAs patterns

Solvent system also plays a vital role on controlling the honeycomb micro porous film structure.[33] In this study, well-ordered pores with narrow size distribution are easily generated using chloroform as a solvent [Fig. 8(A,a)], while it is more difficult using ethyl acetate as a solvent [Fig. 8(B,b)].

As we know, chloroform (density ~ 1.5 g cm^{-3}) is heavier than water while ethyl acetate (density ~

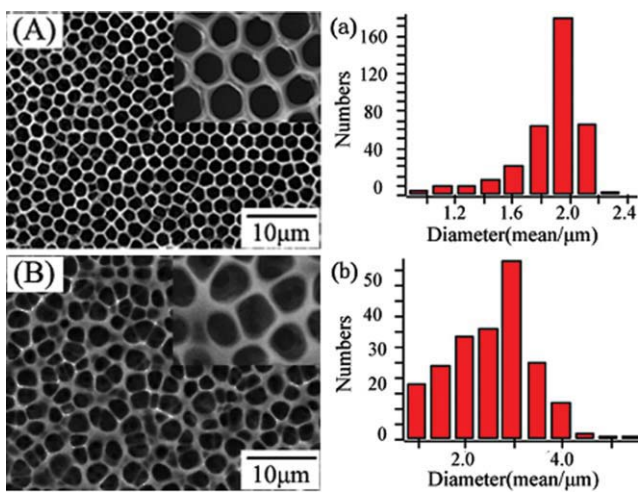

Figure 8 The SEM surface images and their average pore diameter distribution diagrams of the films made by PVB/chloroform (A) and ethyl acetate solution (B) (0.04 g mL^{-1}) at the presence of nitrogen airflow under humidity of 75.1% ± 0.2% for 20 s. [Color figure can be viewed in the online issue, which is available at wileyonlinelibrary.com.]

0.90 g cm^{-3}) is lighter than water; however, the boiling point of chloroform ($\sim$ 61.6°C) is lower than that of ethyl acetate ($\sim$ 77.1°C). Compared to ethyl acetate, chloroform evaporates faster, hence results in bigger temperature gradient between film surface and the atmosphere, this makes more water droplets condensed on the liquid film and increases the thermocapillary convective motion between the interfaces. Considering their density in an order of chloroform > water > ethyl acetate, water droplets are easier to sustain their shapes on a heavier solution than those on a lighter solution. As a result, well-ordered pores are formed on the film surface by using chloroform [Fig. 8(A)]. The solubility[36,37] may be another parameter in explaining the solvent functions on BFAs formation. It is difficult to determine the difference in solubility of PVB in chloroform and ethyl acetate at such a dilute solution. Supposing that the solubility of PVB in chloroform is better than that of PVB in ethyl acetate, in this scenario, PVB polymer chains are able to stay more freely in chloroform, this increases the interacting chances of polar side group with water droplets.[38] Furthermore, since PVB polymer chains can be distributed more evenly in the liquid film, this interaction may exist evenly on the interfaces to support and stabilize the droplets, thus well-ordered honeycomb microporous films can be formed [Fig. 8(A)]. However, the solubility of PVB in ethyl acetate may be relatively poorer, PVB polymer chains are not stretched enough and not be well distributed in the liquid film, resulting in the difference in interactions of water droplets with liquid film at different areas, thus increase the difficulty to obtain well-ordered honeycomb microporous films [Fig. 8(B)].

CONCLUSIONS

Micro porous PVB films with various sizes and distributions have been successfully fabricated from dilute solutions of PVB in chloroform and ethyl acetate by breath figure method. We have controlled the humidity by super saturated salt solution, which is more accurate and convenient. Among various factors, we have found that solvent is the most important factor in obtaining BFAs pattern on PVB films. We have used the solvent parameters including boiling point, density, and their solubility to interpret the mechanism of pore formation. Lower boiling point results in the increase in temperature gradient during faster evaporation while higher density provides stronger support to sustain the shape of water droplets. Solubility may be one of the most important factors in influencing the BAs formation. Higher mobility of polymer chains in a good solvent makes it possible to improve polar chains interaction with water droplets such that regular shape micropores can be obtained.

References

1. Guizard, C.; Princivalle, A. Catal Today 2009, 146, 367.
2. Zhang, Y.; Wang, C. Adv Mater 2007, 19, 913.
3. Li, X. F.; Wang, Y.; Zhang, L.; Tan, S. X.; Yu, X. L.; Zhao, N.; Chen, G. Q.; Xu J. J Colloid Interface Sci 2010, 350, 253.
4. Bindu, P. N.; Chorappan, P. Langmuir 2010, 26, 12948.
5. Wang, C.; Wang, Q.; Wang, T. Langmuir 2010, 26, 1835.
6. Häuβler, M.; Qin, A.; Tang, B. Z. Polymer 2007, 48, 6181.
7. Holland, B. T.; Blanford, C. F.; Stein, A. Science 1998, 281, 538.
8. Bohn, J. J.; Moshe, M. B.; Tikhonov, A.; Qu, D.; Lamont, D. N.; Asher, S. A. J Colloid Interface Sci 2010, 344, 298.
9. Templin, M.; Franck, A.; Du, C. A.; Leist, H.; Zhang, Y. M.; Ulrich, R.; Schädler, V.; Wiesner, U. Science 1997, 278, 1795.
10. Bu, X. Y.; Yuan, J. H.; Song, J. X.; Han, D. X.; Niu, L. Mater Chem Phys 2009, 116, 153.
11. Falcaro, P.; Bertolo, M. J.; Innocenzi, P.; Amenitsch, H.; Bearzotti, A. J Sol-Gel Sci Technol 2004, 32, 107.
12. Higgins, S.; Kennard, R.; Hill, N.; DiCarlo, J.; DeSisto, W. J. J Membr Sci 2006, 279, 669.
13. Park, S. H.; Yin, P.; Liu, Y.; Reif, J. H.; LaBean, T. H.; Yan, H. Nano Lett 2005, 5, 729.
14. Widawski, G.; Rawiso, M.; François, B. Nature 1994, 369, 387.
15. Park, M. S.; Kim, J. K. Langmuir 2005, 21, 11404.
16. Nishikawa, T.; Ookura, R.; Nishida, J.; Arai, K.; Hayashi, J.; Kurono, N.; Sawadaishi, T.; Hara, M.; Shimomura, M. Langmuir 2002, 18, 5734.
17. Kasai, W.; Kondo, T. Macromol Biosci 2004, 4, 17.
18. Bormashenko, E.; Pogreb, R.; Musin, A.; Stanevsky, O.; Bormashenko, Y.; Whyman, G.; Barkay, Z. J Colloid Interface Sci 2006, 300, 293.
19. Zhao, B. H.; Li, C. X.; Lu, Y.; Wang, X. D.; Liu, Z. L.; Zhang, J. Polymer 2005, 46, 9508.
20. Pitois, O.; Francois, B. Colloid Polym Sci 1999, 277, 574.
21. De Boer, B.; Stalmach, U.; Van Hutten, P. F.; Melzer, C.; Krasnikov, V. V.; Hadziioannou, G. Polymer 2001, 42, 9097.
22. Guerrero, M. H.; Thomas, P. D.; Kowollik, C. B.; Stenzel, M. H. Eur Polym J 2005, 41, 2264.
23. Peng, J.; Han, Y. C.; Yang, Y. M.; Li, B. Y. Polymer 2004, 45, 447.
24. Peng, J.; Han, Y. C.; Fu, J.; Yang, Y. M.; L, B. Y. Macromol Chem Phys 2003, 204, 125.
25. Zhao, X. Y.; Cai, Q.; Shi, G. X.; Shi, Y. Q.; Chen, G. W. J Appl Polym Sci 2003, 90, 1846.
26. Yabu, H.; Tanaka, M.; Ijiro, K.; Shimomura, M. Langmuir 2003, 19, 6297.
27. Ejima, H.; Iwata, T.; Yoshie, N. Macromolecules 2008, 41, 9846.
28. Bunz, U. H. F. Adv Mater 2006, 18, 973.
29. Park, M. S.; Kim, J. K. Langmuir 2004, 20, 5347.
30. Reisfeld, R.; Levchenko, V.; Saraidarov, T. Polym Adv Technol 2011, 22, 60.
31. Xu, J.; Li, Y.; Liu, B.; Zhu, M.; Ge, D. Compos Part B 2011, 42, 302.
32. Govor, L. V.; Bashmakov, I. A.; Kaputski, F. N.; Pientka, M.; Parisi, J. Macromol Chem Phys 2000, 201, 2721.
33. Srinivasarao, M.; Collings, D.; Philips, A.; Patel, S. Science 2001, 292, 79.
34. Song, L.; Bly, R. K.; Wilson, J. N.; Bakbak, S.; Park, J. O.; Srinivasarao, M.; Bunz, U. H. F. Adv Mater 2004, 16, 115.
35. Tian, Y.; Ding, H. Y.; Jiao, Q. Z.; Shi, Y. Q. Macromol Chem Phys 2006, 207, 545.
36. Wypych, G. Handbook of Solvents; Chem. Tec. Publishing: Toronto, 2001.
37. Bordes, C.; Fréville, V.; Ruffin, E.; Marote, P.; Gauvrit, J. Y.; Briançon, S.; Lantéri, P. Int J Pharm 2010, 383, 236.
38. Yunus, S.; Delcorte, A.; Poleunis, C.; Bertrand, P.; Bolognesi, A.; Botta, C. Adv Mater 2007, 17, 1079.